Journal of Engineering and Technological Sciences

Research Paper

Photocatalytic Simulation of Phenol Waste Degradation Using Titanium Dioxide (TiO_2) P25-Based Photocatalysts

Wibawa Hendra Saputera[1,2,3,*], Jeffry Jaya Pranata[1], Reynaldo Jonatan[1], Pramujo Widiatmoko[1] & Dwiwahju Sasongko[1]

[1]Research Group on Energy and Chemical Engineering Processing System, Department of Chemical Engineering, Institut Teknologi Bandung, Jalan Ganesa No. 10, Bandung, West Java, 40132, Indonesia
[2]Center for Catalysis and Reaction Engineering, Institut Teknologi Bandung, Jalan Ganesa No. 10, Bandung, West Java, 40132, Indonesia
[3]Research Center for New and Renewable Energy, Institut Teknologi Bandung, Jalan Ganesa No. 10, Bandung, West Java, 40132, Indonesia.

Corresponding author: whsaputera@itb.ac.id

Abstract

Phenol waste treatment is vital in industries such as polymer production, coal gasification, refinery, and coke production. Photocatalytic technology using semiconductor materials offers an effective and ecofriendly approach to degrade phenol. TiO_2 P25 is a widely used photocatalyst, known for its cost-effectiveness, favorable optical and electronic properties, high photoactivity, and photostability. The PHOTOREAC application, a recently developed MATLAB-based software, simulates the degradation of phenol using visible light. A study that combines existing literature and research revealed that pH significantly influences photocatalytic activity, with an optimum pH of 7 for TiO_2 P25-mediated phenol degradation. The recommended photocatalyst concentration ranged from 0 to 10 g/L for reactor volumes between 25 and 60 mL, and from 0 to 5 g/L for 100-mL reactors. Phenol wastewater volume and light intensity also impact degradation efficiency. Adequate oxygen supply, achieved through bubbling and mixing, is essential for the formation of radical compounds. The Ballari kinetic model proved to be the most suitable for phenol degradation with TiO_2 P25. Thus, by combining PHOTOREAC simulations with experimental data, the treatment process could be optimized to achieve higher degradation efficiency and estimate the treatment time for specific waste degradation levels. This study contributes to the advancement of phenol waste treatment and the development of improved photocatalytic wastewater treatment technologies.

Keywords: *MATLAB; Photocatalytic; phenol; PHOTOREAC; TiO_2 P25; waste treatment.*

Introduction

Industrial wastewater pollution has significant adverse effects on the environment. Phenol, an organic pollutant commonly found in industrial wastewater, poses serious risks to both human health and the environment due to its toxic, corrosive, and mutagenic properties [1]. Various methods, such as chemical oxidation, adsorption, and biotechnology, have been explored for the removal of phenolic compounds from wastewater [2,3]. However, these conventional approaches have limitations and drawbacks [4]. In recent years, significant advancements have been made in the development of technologies aimed at treating phenol waste in industrial wastewater, overcoming the limitations of traditional methods.

Photocatalysis is one such technology used for industrial wastewater treatment [5], which can decompose organic compounds, including phenol, into environmentally harmless substances: water and carbon dioxide gas. This process employs semiconductors as key components [6]. Semiconductors possess a conduction band and a valence band with an appropriate band gap. When exposed to light energy, electrons in the valence band become excited and move to the conduction band, creating holes in the process. The separation of electrons and holes promotes the formation of hydroxyl radical compounds (•OH) and superoxide ($\bullet O_2$-), which play a crucial role in the degradation of organic waste. Titanium dioxide (TiO_2) is a widely used semiconductor photocatalyst due to its photochemical stability and high efficiency [7]. However, TiO_2 exhibits a relatively high

ISSN: 2337-5779
J. Eng. Technol. Sci. Vol. 55, No. 3, 2023, 419-433
DOI: 10.5614/j.eng.technol.sci.2023.55.4.6

band gap (between 3.0 to 3.2 eV) [8], resulting in limited absorption of visible light. Furthermore, the recombination time between holes and electrons is fast, diminishing the efficiency of photocatalytic degradation. It is essential to emphasize that the photocatalytic activity is influenced by various factors. Therefore, a comprehensive evaluation of operating conditions [9,10] and catalyst characteristics [9,11] is necessary to enhance the efficiency of waste degradation. Some recent studies have shown that altering the characteristics of semiconductor materials can impact the photocatalytic activity, such as modifying the semiconductor material with heterojunctions [12-14], metals and non-metals [15-21] as well as surface modifications [22-26]. Although numerous experimental studies have investigated the efficiency and performance of various photocatalytic materials for wastewater treatment, there is a lack of comprehensive understanding regarding the underlying affecting factors and appropriate kinetic model validated via simulation. This gap makes it challenging to optimize and design novel photocatalysts with enhanced properties.

Thus, this study aimed to investigate the impact of several factors on photocatalytic activity, including pH, initial phenol concentration and volume, catalyst characteristics, light intensity, and catalyst doping. Additionally, the study evaluated the most suitable kinetic model for phenol waste degradation through photocatalysis. The analysis was conducted through the combination of a literature review and simulation using the PHOTOREAC software, a recently developed tool that calculates the overall photon absorption (OVRPA) in catalytic processes and models photocatalytic activity using four kinetic equations: Langmuir-Hinshelwood, Zalazar, Ballari, and Mueses kinetic models. The variation in these factors relies heavily on a secondary database consisting of photocatalytic degradation experiments conducted by other researchers.

Research Methodology

Initial Preparation Stage

The search for a suitable simulator to model the photocatalytic process was conducted during the initial preparation stage of this research. After careful consideration, the PHOTOREAC software, a MATLAB-based program capable of simulating photocatalysis using a visible light source, was selected. The software was obtained through Professor Miguel Mueses from the University of Cartagena, Colombia.

The PHOTOREAC software was used to determine the photon absorption (OVRPA) in the photocatalytic process and to model the photocatalytic reactions using the available kinetic model database. The software offers four kinetic models that can best fit the reaction kinetics data, namely Langmuir-Hinshelwood, Zalazar, Ballari, and Mueses kinetic models, whose formulas are shown by Eqs. (1)-(4) respectively [27].

$$(-r_i)V_R = -K_{kin} \times k^{L-H} \times \frac{C_i}{1+k^{L-H}C_i} \times (E_g)^{0,5} \quad (1)$$

$$(-r_i)V_R = \frac{\Phi_g^{eff} \times E_g}{\frac{1}{2}+\left[\frac{1}{4}+K_{kin}\times\frac{\Phi_g^{eff}}{2\times C_{cat}^2\times C_i\times C_{O2}}\right]^{0,5}} \quad (2)$$

$$(-r_i)V_R = -2\frac{\alpha_1}{\kappa_p} \times \left[-1+\sqrt{1+\kappa_p\frac{\alpha_2 E_g}{C_i}}\right] \times C_i \quad (3)$$

$$(-r_i)V_R = -2\frac{\alpha_1}{\kappa_p} \times \left[-1+\sqrt{1+\frac{\kappa_p}{\alpha_1}\Phi_g^{eff}E_g}\right] \times \frac{k^{L-H}C_i}{1+k^{L-H}C_i} \quad (4)$$

It is important to note that the PHOTOREAC software that was utilized in this study was still in the development stage, which imposed certain limitations on its use. These limitations encompass two main aspects: (i) the simulation only allows for the utilization of TiO_2 P25 as the photocatalyst, and (ii) the light source utilized in the simulation is restricted to sunlight or a xenon Lamp. Moreover, the PHOTOREAC software relies on several assumptions to solve the differential equations and derive the kinetic parameters. These assumptions include: (i) no mass transfer limitations, (ii) considering convection and diffusion as a centralized system (lumped system), and (iii) assuming differential conversion per pass.

DOI: 10.5614/j.eng.technol.sci.2023.55.4.6

In parallel, secondary data for the simulation were gathered through an extensive review of scientific literature encompassing previous experimental studies. The selection criteria for the secondary data included the following parameters: (i) utilization of TiO_2 P25 as the photocatalyst, (ii) employment of direct sunlight or a xenon lamp as the light source, (iii) degradation of phenol as the targeted waste, and (iv) clearly defined reactor volume and waste volume in the secondary data. In the event of incomplete secondary data, certain assumptions are made, such as: (i) assuming the dimensions of the photoreactor to be those of a commercial quartz beaker glass if actual dimensions are unknown, (ii) assuming an energy density of 1000 W/m^2 and 300 W/m^2 for light intensities produced by 1,000-W and 300-W lamp sources, respectively, and (iii) assuming a pH value within the range of 5 to 6 if no specific information regarding the pH level is available.

Xenon lamps can be considered viable light sources due to their wavelengths, which closely resemble those of sunlight [28]. The obtained secondary data were categorized into two groups based on the diffused light intensity: of 1,000 W/m^2 (Data A to C) and 300 W/m^2 (Data D to G). The sources of the journals from which the secondary data were derived are presented in Table 1.

Table 1 List of secondary data sources.

Data	Journal Name, Volume, Page	References
A	Industrial and Engineering Chemistry Research, 53, 18824-18832	[29]
B	Physicochemical Problems and Mineral Processing, 46, 21-30	[30]
C	Separation and Purification Technology, 72, 309-318	[31]
D	Journal of Hazardous Materials, 152, 48-55	[32]
E	Scientific Reports, 8, 1-10	[33]
F	Applied Catalysis B: Environmental, 144, 893-899	[34]
G	Catalysis Today, 335, 101-109	[35]

Simulation Stage

The collected secondary data were simulated using the PHOTOREAC software. The simulation results from PHOTOREAC provide important parameters for the analysis, including the photon absorption inside the photoreactor, which is quantified by the Overall Volumetric Rate of Photon Absorption (OVRPA) value. Additionally, the most suitable kinetic model for the phenol photocatalytic degradation process is determined based on the R^2 value. The search for the optimal kinetic model involves employing a non-linear regression procedure. The error function utilized in this procedure is defined as the sum of squared errors between the experimental water contaminant concentration ($C_{i,exp}$) and the concentration value obtained from the numerial solution of Eq. (5)($C_{i,\,calc}$) [27].

$$F_{obj} = \sum_{i=1}^{N} \left(C_{i,exp} - C_{i,calc}\right)^2 \quad (5)$$

The simulation of the kinetic model in PHOTOREAC enables the identification of the most suitable equation model for the degradation process of phenol using TiO_2 P25. The available kinetic equation models in PHOTOREAC include Langmuir-Hinshelwood, Zalazar, Ballari, and Mueses kinetic models.

To perform a simulation in PHOTOREAC, several data inputs from the photocatalytic experiment are required. These inputs consist of the photoreactor type, photoreactor dimensions, reaction volume (in liters), photocatalyst concentration, irradiation light source intensity (in W/m^2), and photocatalytic degradation activity. These data inputs can be obtained from the secondary data collected from previous experiments.

Three options for photoreactor types are available: Compound Parabolic Collectors (CPC), Offset Multi Tubular Photoreactor (OMTP), and Flat Plate Photoreactor (FPP). The selection of the photoreactor type depends on the specific photoreactors used in the secondary data experiments. The photoreactor configurations can be observed in Figure 1.

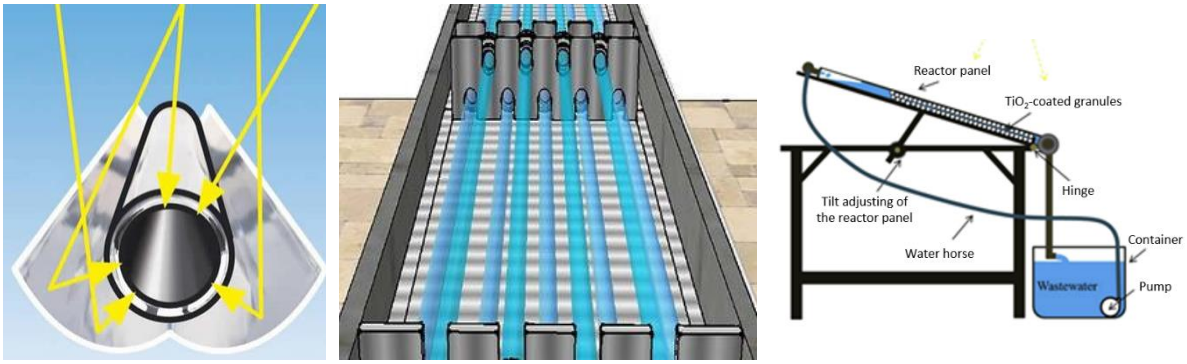

(a) (b) (c)

Figure 1 Photoreactor configuration types: (a) compound parabolic collectors [36], (b) offset multi-tubular reactor [37], (c) flat plate photoreactor [38].

The PHOTOREAC software calculates the OVRPA value by averaging the Local Volumetric Rate of Photon Absorption (LVRPA) within the photoreactor. The LVRPA values at different positions inside the photoreactor are determined by evaluating the light intensity using the radiative transfer equation (RTE) given in Eq. (6) [39]:

$$\frac{dI_\lambda(S,\Omega)}{dS} = -K_\lambda \times I_\lambda(S,\Omega) - \sigma_\lambda \times I_\lambda(S,\Omega) + \frac{\sigma_\lambda}{4\pi}\int p(\Omega' \rightarrow \Omega) \times I_\lambda(s,\Omega')d\Omega' \quad (6)$$

One of the efficient and expedient methods for solving the RTE is the Six Flux Absorption Scattering Model (SFM). SFM simplifies the photon distribution by considering movement along six Cartesian coordinate directions: forward (pf), backward (pb), and perpendicular (ps). These directional movements are approximated within the SFM using two approaches: the Diffuse Reflectance (DR) approach and the Henyey-Greenstein (HG) approach [39].

In the DR approach, the values of pf, pb, and ps are 0.11, 0.71, and 0.045, respectively. On the other hand, the HG approach employs a formula to calculate the values of pf, pb, and ps. For the purpose of this research, the SFM-HG approach was utilized to calculate the OVRPA value, as it offers improved accuracy compared to the SFM-DR approach in determining the OVRPA [39].

Analysis Stage

The analysis of both the secondary data literature and the results obtained from the simulation using the PHOTOREAC software enabled the examination of various phenomena occurring during the photocatalytic process. The findings were categorized into two key factors that influence the efficiency of waste degradation through photocatalysis: operating conditions and photocatalyst characteristics.

Regarding the operating conditions, this study analyzed the following factors: (i) pH level, (ii) photocatalyst concentration, (iii) initial concentration and volume of the waste, (iv) light intensity, (v) duration of irradiation, and (vi) special treatment in the form of a bubbling process. These operating conditions play a significant role in the photocatalytic process and were thoroughly investigated.

Furthermore, the characteristics of the photocatalyst to be analyzed in this study included the surface area of the photocatalyst as well as the band gap and crystallinity. These characteristics significantly impact the photocatalytic activity and were assessed to understand their influence on the degradation of phenol through the TiO_2 P25 photocatalytic process.

Additionally, the results obtained from the simulation of the kinetic models were analyzed to identify the most suitable kinetic model for the degradation of phenol using the TiO_2 P25 photocatalyst. This analysis was expected to contribute to a better understanding of the overall photocatalytic mechanism involved in phenol degradation and aid in optimizing the efficiency of the process.

DOI: 10.5614/j.eng.technol.sci.2023.55.4.6

Result and Discussion

Effect of Operating Conditions

pH

Changes in the pH of the waste solution can significantly influence the performance of photocatalytic degradation. The charge on the compound surface is determined by the point of zero charge (pzc) of the photocatalyst compound. When the pH of the solution is below the pzc value, the compound surface becomes positively charged, whereas a pH above the pzc value results in a negative charge on the surface. This charge distribution directly affects the adsorption process between the photocatalyst and the contaminant compound, consequently influencing the efficiency of photocatalytic degradation [40].

To analyze the effect of pH, data from experiments B, C, and G were utilized. Experiment B was conducted at pH 7, experiment C at pH 5-6, and experiment G at pH 2. Based on Table 2, it is evident that the degradation performance in experiment B was superior to that in experiment C. This can be attributed to the fact that at pH 7, TiO_2 carries a negative charge/deprotonated state due to its pzc value of approximately ±6.25 [41], while the phenol surface remains positively charged/protonated at pH 7. The pzc value of TiO_2 is determined by calculating the average pK values, with pKa_1 at 4.5 and pKa_2 at 8.0 [42]. The difference in surface charge leads to a significant enhancement in photocatalytic degradation performance [40].

Furthermore, experiment G exhibited the poorest photocatalytic degradation performance, which was carried out at pH 2.0. This phenomenon can be explained by a similar reasoning to using a solution with pH greater than 7. As long as there is a difference in charge between the surface of the photocatalyst and the waste, the degradation efficiency is improved. In a highly alkaline solution, where both the phenol and TiO_2 surfaces are negatively charged, they repel each other, resulting in a significant drop in degradation performance [40].

Table 2 Comparison of operating conditions, photocatalyst characteristics, degradation efficiency, and OVRPA value for Data B, C, and G.

Data	Degradation at 60 minutes (%)	pH	Initial Phenol Concentration (ppm)	Waste Volume (mL)	Photocatalyst Concentration (g/L)	Photocatalyst Surface Area (m^2/g)	OVRPA SFM-DR (W/m^3)
B	26.00	7	19.76	25	5	50.00	670,051
C	9.98	5-6	19.70	25	5	59.00	670,051
G	4.50	2	10.00	50	1	241.32	246,158

Photocatalyst Concentration

The OVRPA value is directly influenced by the photocatalyst concentration in the photoreactor, measured in g/L units. The OVRPA value (Eg) plays a crucial role in determining the efficiency of photocatalytic degradation of phenol waste, as the kinetic reaction rate is directly proportional to the OVRPA value, as represented by Eqs. (1) to (4).

Increasing the amount of photocatalyst can enhance the performance of photocatalytic waste degradation by providing more active sites for waste adsorption and light absorption within the photocatalyst. However, this synergistic effect of increasing the photocatalyst amount is limited to a certain extent. Beyond this threshold, the photocatalyst particles may agglomerate, leading to limitations in light penetration and waste adsorption [29,43].

To examine the impact of photocatalyst concentration on OVRPA, PHOTOREAC simulations were employed. The simulation results are depicted in Figure 2, allowing for a comparison of the effect of photocatalyst concentration on OVRPA.

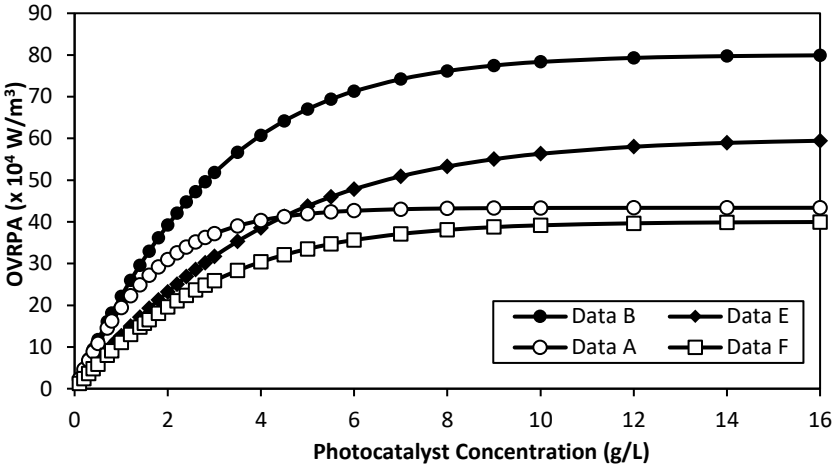

Figure 2 Effect of photocatalyst concentration on OVRPA using PHOTOREAC simulation with Data A, B, E, and F.

The findings presented in Figure 2 demonstrate a significant increase in the OVRPA value within a specific concentration range, depending on the volume of the reactor or the volume of waste. However, beyond this range, the increase in the OVRPA value becomes less pronounced and eventually reaches a plateau.

For instance, in Data A and Data F, with a reactor volume of 100 mL, the plateau point is attained when the photocatalyst concentration exceeds 5 g/L. Conversely, in Data B and Data E, with reactor volumes of 25 mL and 60 mL respectively, the plateau point is reached after the photocatalyst concentration surpasses 10 g/L. The difference in the plateau points can be attributed to variations in light penetration between the large and small photoreactors, with the larger photoreactor exhibiting poorer light penetration.

Based on this analysis, it can be concluded that changes in the volume of waste will impact the optimal photocatalyst concentration [44], which suggests that as the volume of waste increases, the optimal photocatalyst concentration decreases.

Initial Waste Concentration and Volume

The initial concentration of the waste solution is a significant factor that influences the degradation process. A higher initial concentration of the waste solution leads to a longer degradation time due to the increased amount of waste adsorbed on the photocatalyst surface. This, in turn, reduces the formation of hydroxyl radicals (HO•), which play a crucial role in the degradation process. Additionally, a high concentration of waste reduces the penetration of light to the photocatalyst, thereby diminishing the photocatalytic degradation performance [43].

To examine the effect of the waste's initial concentration on photocatalytic degradation performance, a comparison was made between Data A and Data B, as presented in Table 3. Theoretically, a high initial concentration of the waste solution results in increased turbidity, which hampers the distribution of photons within the photoreactor. However, based on Data A and Data B, it can be observed that the impact of the initial concentration of phenol is not as significant as that of the photocatalyst concentration. Therefore, while the initial concentration of the waste solution does have an influence on the degradation process, its effect is not as pronounced as that of the photocatalyst concentration.

DOI: 10.5614/j.eng.technol.sci.2023.55.4.6

Table 3 Comparison of operating conditions, photocatalyst characteristics, degradation efficiency, and OVRPA value for Data A and B.

Data	Degradation at 60 minutes (%)	pH	Initial Phenol Concentration (ppm)	Waste Volume (mL)	Photocatalyst Concentration (g/L)	Photocatalyst Surface Area (m^2/g)	Anatase / Rutile Ratio	OVRPA SFM-DR (W/m^3)
A	26.30	7	40.00	100	1	n.a.	80/20	194,209
B	26.00	7	19.76	25	5	50.00	70/30	670,051

The relationship between the volume of waste and the OVRPA value was investigated through photon distribution simulation using PHOTOREAC. Figure 3 illustrates the effect of waste volume on the OVRPA value in a photoreactor. It can be observed that increasing the volume of waste leads to a decrease in the OVRPA value.

This phenomenon occurs because as the volume of waste to be processed increases, the distribution of photons inside the photoreactor becomes less uniform. Instead of being evenly dispersed, the photons tend to concentrate on the surface directly exposed to the light source. Consequently, the overall OVRPA decreases as the photons are not effectively distributed throughout the entire volume of the waste. Therefore, it can be concluded that a larger volume of waste results in a reduced OVRPA value due to the uneven distribution of photons within the photoreactor.

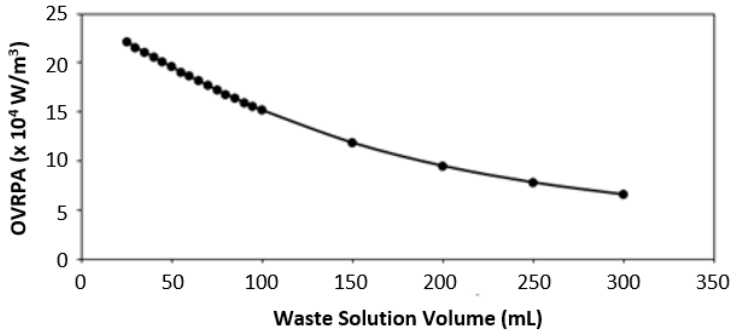

Figure 3 Effect of waste solution volume on the OVRPA value using PHOTOREAC simulator.

Light Intensity

Increasing the light intensity in the photoreactor enhances photon absorption and accelerates the rate of waste degradation. This is evident from the OVRPA values obtained using PHOTOREAC software, as shown in Table 4. Comparing the OVRPA values at different light intensities (1,000 W/m^2 and 300 W/m^2), it is clear that higher light intensity leads to higher OVRPA values, indicating increased photon absorption. Consequently, the photocatalytic degradation process exhibits greater efficiency with higher light intensity due to the availability of more photons for the reaction. Therefore, the variation in light intensity directly affects the OVRPA value, reflecting its impact on photon absorption and the overall effectiveness of waste degradation through photocatalysis.

Table 4 Comparison of operating conditions, photocatalyst characteristics, degradation efficiency, and OVRPA value for Data A, D, and F.

Data	Light Intensity (W/m^2)	Degradation at 60 minutes (%)	Initial Phenol Concentration (ppm)	Photocatalyst Concentration (g/L)	Waste Volume (mL)	pH	Band Gap (eV)	Anatase / Rutile Ratio	OVRPA SFM-DR (W/m^3)
A	1000	26.30	40.00	1.0	100	7.0	3.15	80/20	194,209
D	300	3.90	50.00	1.0	100	5-6	3.20	n.a.	48,526
F	300	19.00	10.00	1.5	100	7.1	n.a.	n.a.	156,394

The increase in light intensity is accompanied by a corresponding increase in the OVRPA value. Among the data presented in Table 4, Data A exhibits the highest degradation percentage after 60 minutes of photocatalytic duration. Despite having a lower initial phenol concentration and a higher photocatalyst concentration, Data A outperformed Data F in terms of degradation efficiency. This superiority can be attributed to the higher OVRPA value achieved in Data A, resulting in a greater production of radical compounds due to enhanced photon absorption. The process of photon absorption triggers the separation of electrons and holes within the semiconductor, leading to the generation of more radical compounds for waste degradation and ultimately enhancing the overall degradation efficiency [40,45,46].

Irradiation Time

In general, an increase in irradiation time leads to higher degradation efficiency. Irradiation time represents the duration of interaction between the photocatalyst and the light source, which is crucial for the production of radical compounds. Longer irradiation times result in extended interactions, allowing for more radical compound generation and consequently enhancing degradation efficiency. The prolonged duration facilitates the formation of radical compounds that play a vital role in the degradation process of organic waste. Additionally, longer irradiation times increase the contact time between the radical compounds and the substrate, leading to further degradation of the organic compounds themselves [40,46], highlighting the positive relationship between irradiation time and degradation efficiency. However, it is important to note that the photocatalytic process is complex and influenced by various factors, such as photocatalyst characteristics, waste concentration, and volume. Therefore, there may be instances where longer durations do not necessarily result in superior degradation compared to shorter durations. Nonetheless, the data presented in Table 5 demonstrate that increasing the irradiation time enhanced waste degradation efficiency under both 1,000 W/m^2 and 300 W/m^2 light intensities.

Table 5 Comparison of light intensity and degradation efficiency for Data A and F.

Data	Light Intensity (W/m^2)	Degradation at 60 minutes (%)	Degradation at 180 minutes (%)
A	1000	26.30	68.63
F	300	19.00	32.00

Special Treatment

Special treatments are often employed in photocatalytic systems to enhance the efficiency of waste degradation. Some commonly used treatments include sonication, bubbling, doping, and coupling. Sonication is typically performed prior to the photodegradation process to achieve even distribution of photocatalyst particles, promoting a homogeneous structure and minimizing particle agglomeration. Agglomeration can impede light penetration, which is crucial for providing energy to the photocatalyst. Additionally, agglomeration reduces the contact surface area of the photocatalyst, compromising its efficiency [47]. Pre-mixing and stirring of the photocatalyst and waste solution in the dark are often employed to establish an adsorption-desorption equilibrium, allowing the photocatalyst to adsorb the waste solution onto its active sites, thereby enhancing degradation performance [48]. Bubbling or aeration is another common treatment in photocatalytic processes, supplying oxygen to facilitate the formation of superoxide radicals by photoelectrons. This presence of bubbling improves the degradation efficiency of organic waste (Table 6). However, even without bubbling, the photocatalytic process can still proceed, suggesting that superoxide radicals are not the sole contributors to organic waste degradation [49], hydroxyl radicals also play a significant role in photocatalytic degradation of phenol [45]. Conversely, Data G exhibits poor degradation performance, likely due to the experimental conditions at a very low pH below the point of zero charge (pzc) of TiO_2. Furthermore, the efficiency of Data C is almost half that of Data E even though both Data C and E have similar pH conditions and Data C has a higher light intensity compared to Data E. This difference can be attributed to the varying concentrations of photocatalyst used in each experiment. Data C utilized a photocatalyst concentration five times higher than Data E. It is important to note that increasing the photocatalyst concentration does not necessarily lead to a proportional increase in efficiency.

DOI: 10.5614/j.eng.technol.sci.2023.55.4.6

Table 6 Comparison of the operating conditions (light intensity, pH, and bubbling) and photocatalytic degradation efficiency of phenol waste for Data A to G.

Data	Light Intensity (W/m^2)	Degradation at 60 minutes (%)	pH	Remarks
A	1000	26.30	7.0	Bubbling
B	1000	26.00	7.0	Bubbling
C	1000	9.98	5.0-6.0	Bubbling
D	300	3.90	5.0-6.0	Without bubbling
E	300	17.00	5.0-6.0	Bubbling
F	300	19.00	7.1	Bubbling
G	300	4.50	2.0	Bubbling

Photocatalyst modification, particularly through doping, is commonly employed to enhance the degradation efficiency of organic waste. Doping introduces a new energy band that is lower than the conduction band of the undoped photocatalyst, thereby reducing the band gap and improving the electrical, optical, and structural properties of the photocatalyst [50]. Consequently, the doping process can expedite the waste degradation duration. Table 7 presents a comparison between the performance of doped and undoped photocatalysts in organic waste degradation. The data reveals that the degradation efficiency is superior when utilizing doped photocatalysts, as the dopant acts as an electron scavenger by capturing and trapping electrons. This prolongs the recombination time between electrons and holes, facilitating the occurrence of radical formation reactions [51].

Table 7 Comparison of photocatalytic degradation efficiency of phenol waste with and without metal/non-metal doping.

Data	Dopant	Degradation without doping (%)	Degradation time without doping (min)	Degradation with doping (%)	Degradation time with doping (min)
A	Graphene	68.63	180	75	180
B	Carbon	26.20	60	55	60
C	Silver	12.60	80	32	80
D	Sulphur	17.00	120	100	60
F	Carbon / Graphene Oxide	32.00	180	96	180

Effect of Photocatalyst Characteristics

Specific Surface Area

A comparison between Data B, C, and G was conducted to assess the impact of surface area on the efficiency of phenol waste degradation, as presented in Table 2. Surprisingly, Data G, which exhibited the largest surface area, did not demonstrate the highest degradation efficiency for phenol waste [52], highlighting that an increase in surface area in powder does not always correspond to enhanced degradation efficiency in the photocatalytic process. The efficiency of waste degradation in photocatalysis is primarily influenced by the presence of active sites on the photocatalyst and the crystal defects within the photocatalyst, rather than solely relying on surface area. It should be noted that an increase in surface area may lead to an abundance of crystalline defects in the photocatalyst, which can promote electron and hole recombination, ultimately reducing photoactivity. To achieve optimal photoactivity, it is crucial to strike a balance between surface area and crystallinity [52].

Crystallinity Phase and Band Gap

The composition of the anatase and rutile phases in TiO_2 has been found to impact the band gap of the photocatalyst. This is due to the difference in band gap between the anatase and rutile phases, with anatase having a band gap of approximately 3.2 eV and rutile having a band gap of around 3.02 eV. When TiO_2 consists of an 80/20 ratio of anatase and rutile phases respectively, it exhibits active absorption in the wavelength range of 384 nm to 410 nm for both phases [52]. It is worth noting that even though TiO_2 P25 is a commercial

photocatalyst, the synthesized TiO_2 P25 may have a different composition in terms of anatase and rutile ratios, as indicated in Table 3.

Kinetic Model Simulation Result

Based on the conducted simulation of the kinetic model, it has been determined that the Ballari kinetic model is suitable for the four data, while the Langmuir-Hinshelwood kinetic model is suitable for the three data. The specific details and results of this analysis can be seen in Table 8.

Table 8 Comparison of kinetics model simulation initial condition and result for Data A to G.

Data	R^2 for Langmuir-Hinshelwood Model	R^2 for Zalazar Model	R^2 for Ballari Model	Initial Phenol Concentration (ppm)	Suitable Kinetics Model
A	0.9903	0.9892	0.9781	40.0	Langmuir-Hinshelwood
B	0.8482	0.8564	0.9057	19.8	Ballari
C	0.9080	0.8533	0.9037	19.7	Langmuir-Hinshelwood
D	0.9449	0.9413	0.9348	50.0	Langmuir-Hinshelwood
E	0.8553	0.4813	0.8788	13.5	Ballari
F	0.8783	0.8369	0.9334	10.0	Ballari
G	0.6962	0.6250	0.8033	10.0	Ballari

The application of Mueses' equation for modeling the photocatalytic degradation of phenol using TiO_2 was found to be unsuitable. The simulation results demonstrate significant deviations from alternative equation models, indicating that the predictions from this model are not accurate. As a result, the Mueses model is not included in further analysis or consideration.

The PHOTOREAC kinetic simulation analysis revealed that the Langmuir-Hinshelwood (L-H) and Ballari kinetic models exhibited the best fitting for all seven data sets. The analysis in Table 8 demonstrates a trend indicating the suitability of different kinetic models for varying initial concentrations of phenol. The L-H model tends to be more suitable for high initial phenol concentrations, while the Ballari model is more appropriate for lower initial concentrations. This distinction arises from the initial assumption of the Ballari model, which simplifies waste concentration with lower values. It is worth noting that even when the L-H model exhibited better fittings than the Ballari model, the differences in fitting values between the two models are not substantial, as evidenced by the R^2 values in Data A, C, and D. Therefore, the Ballari kinetic model can generally be employed to model the degradation of phenol waste using TiO_2 P25, regardless of whether the phenol concentration is high or low.

To further compare the kinetic parameter values, the Ballari kinetic simulation model was utilized, focusing on the α_1 and α_2 values. The simulation results demonstrate that the values of α_1 and α_2 are influenced by the photocatalytic degradation performance and the OVRPA value. In general, as the photocatalytic degradation performance decreases, the value of $\alpha 1$ also decreases, while the value of α_2 increases. Additionally, an increase in the OVRPA value leads to a decrease in the α_2 value since α_2 functions as a correction factor for OVRPA [53]. The comparison of the kinetic simulation can be observed in Table 9, where the simulation was conducted with 1,000 W radiation using the Ballari kinetic model.

Table 9 Comparison of kinetic parameter values (α_1 and α_2), operating condition, photocatalyst characteristic, and photocatalytic degradation efficiency for Data A, B, and C.

Data	Degradation at 60 minutes (%)	Initial Phenol Concentration (ppm)	OVRPA SFM-HG (W/m^3)	α_1	α_2	Photocatalyst Surface Area (m^2/g)
A	26.3	40.0	194,209	6.61×10^{-7}	0.33548	n.a.
B	26.0	19.8	670,051	5.79×10^{-6}	0.02042	50
C	10.0	19.7	670,051	1.42×10^{-6}	0.02225	59

The value of α_1 for Data A is smaller than that of Data B, which can be attributed to the structure of the Ballari equation. When the degradation rate is held constant, an increase in the initial concentration of phenol will lead to a smaller α_1 value. This finding aligns with the observations in Data A and Data B, where Data A had a higher

DOI: 10.5614/j.eng.technol.sci.2023.55.4.6

initial phenol concentration compared to Data B, while both exhibited the same photocatalytic degradation performance. Additionally, the OVRPA value in Data B was significantly larger than in Data A, and the α_2 value in Data B was lower than in Data A, which is in line with the existing literature.

The Langmuir-Hinshelwood model has a good fit for some data because the Langmuir-Hinshelwood model is a general equation to model the kinetic rate for catalytic reaction. Because of it, the Langmuir Hinshelwood model is suitable for most catalytic reactions (photocatalytic reaction included), except there are some differences/disturbances in the adsorption process between the substrate and the catalyst. In this case, the substrate is phenol and the catalyst is TiO_2. It can be seen from Data G that the R^2 for the Langmuir-Hinshelwood model was much lower compared to Ballari, because the photocatalytic reaction takes place in an acidic environment and therefore the adsorption process between phenol and TiO_2 is disturbed.

Conclusion

The efficiency of phenol waste degradation is influenced by various operational conditions and photocatalyst properties. One of the key factors is the pH value, with a pH of 7 being optimal for the photocatalysis process. The amount of photocatalyst used also has an impact on the OVRPA value, contact surface area, and turbidity of the effluent solution. An optimal photocatalyst concentration range of 0 to 5 g/L is recommended for a waste volume of 100 mL, while a range of 0-10 g/L is suitable for volumes of 25 to 60 mL. The initial effluent concentration is another important parameter that affects the OVRPA value and turbidity, with the optimal value depending on other process parameters. The waste volume and light intensity are additional factors that influence the OVRPA value. Increasing the waste volume can lead to uneven photon distribution within the photoreactor, resulting in a decrease in the OVRPA value. As for light intensity, the increment can theoretically increase the photon absorption and the degradation rate.

The bubbling process, which provides oxygen, is necessary for achieving optimal degradation efficiency of phenol waste. Bubbling helps in the formation of superoxide radicals, contributing to the degradation process. However, the presence of superoxide radicals is not the sole factor affecting organic waste degradation, as hydroxyl radicals also play a significant role. Photocatalyst properties, such as the composition of rutile and anatase phases, influence the band gap, which is crucial for the separation of electrons and holes. Doping the photocatalyst enhances the degradation performance by acting as an electron scavengers, reducing rapid recombination. The surface area of the photocatalyst affects waste adsorption and interaction with the light source, influencing the overall efficiency. Based on kinetic modeling, the Ballari kinetic model is deemed the most suitable for modeling the degradation process of phenol waste using TiO_2 P25 photocatalyst. This model provides a good fit to the experimental data and can be utilized for further analysis and optimization. Overall, the PHOTOREAC simulation proved to be a valuable tool for researchers and practitioners in the field of photocatalytic wastewater treatment. It enables the investigation of various operational conditions and photocatalyst properties, contributing to the development of more effective and efficient treatment technologies.

Acknowledgments

This research was supported by the Indonesian Ministry of Education, Culture, Research, and Technology Research Program 2023 (Grant No. 110/E5/PG.02.00/PL/2023). The invaluable support and collaboration of Professor Miguel from the University of Cartagena, Colombia, have played a significant role in the success of this study. Special thanks to Professor Miguel Mueses for providing access to the PHOTOREAC software, which served as the fundamental tool in conducting this research.

Nomenclature

C_{cat}	=	Photocatalyst concentration [kg/m^3]
C_i	=	Contaminant concentration in the solution [mol/m^3]
$C_{i,\,calc}$	=	Calculated water contaminant concentration [mol/m^3]
$C_{i,\,exp}$	=	Experimental water contaminant concentration [mol/m^3]

C_{O2} = Oxygen concentration[mol/m^3]
E_g = Overall Volumetric Rate of Photon Absorption (OVRPA) [W/m^3]
I_λ = Photon irradiation[W/sr]
K_{kin} = Kinetic constant for Langmuir-Hinshelwood and Zalazar kinetic model [mol.s.kg^2/m^{-9}]
$k^{L\text{-}H}$ = Kinetic constant for Langmuir-Hinshelwood [m^3/mol]
p_b = Backward photon scattering direction [-]
p_f = Forward photon scattering direction [-]
p_s = Perpendicular photon scattering direction [-]
S = Spatial coordinate [-]
V_R = Reactor volume [m^3]
α_1 = Kinetic constant for Ballari and Mueses kinetic model [cm/s]
α_2 = Kinetic constant for Ballari kinetic model [mol/watt.cm]
κ_λ = Absorption coefficient [-]
κ_p = Particle constant [m^3/m^2]
Ω = Solid angle direction [-]
Φ_g^{eff} = Effective quantum yield [mol/s.watt]

References

[1] World Health Organization, *International Programme on Chemical, Phenol: Health and Safety Guide*, World Health Organization: Geneva, 1994.

[2] Sacco, O., Vaiano, V., Daniel, C., Navarra, W., & Venditto, V. *Removal of Phenol in Aqueous Media by N-Doped TiO_2 Based Photocatalytic Aerogels*. Materials Science in Semiconductor Processing, **80**, pp. 104-110, 2018. doi: 10.1016/j.mssp.2018.02.032.

[3] Saputera, W.H., Putrie, A.S., Esmailpour, A.A., Sasongko, D., Suendo, V. & Mukti, R., *Technology Advances in Phenol Removals: Current Progress and Future Perspectives*. Catalysts, **11**(8), 998, 2021. doi: 10.3390/catal11080998.

[4] Royaee, S.J. & Sohrabi, M., *Application of Photo-Impinging Streams Reactor in Degradation of Phenol in Aqueous Phase*. Desalination, **253**(1), pp. 57-61, 2010. doi: 10.1016/j.desal.2009.11.033.

[5] Tetteh, E.K., Rathilal, S. & Naidoo, D.B., *Photocatalytic Degradation of Oily Waste and Phenol from A Local South Africa Oil Refinery Wastewater Using Response Methodology*. Scientific Reports, **10**(1), pp. 1-12, 2020. doi: 10.1038/s41598-020-65480-5.

[6] Bilya, M.A. & Sani, M.H., *Determination of the Band-Gap of a Semiconductor: Germanium Chip Using Four Probe Set-Up*. International Journal of Science and Research, **5**(2), pp. 1137-1140, 2016. doi: 10.21275/v5i2.nov161376.

[7] Dragana Štrbac, D., Aggelopoulos, C.A., Štrbac, G., Dimitropoulos, M., Novaković, M., Ivetić, T. & Yannopoulos, S.N., *Photocatalytic Degradation of Naproxen and Methylene blue: Comparison Between ZnO, TiO_2 and Their Mixture*. Process Safety and Environmental Protection, **113**, pp. 174-183, 2018. doi: 10.1016/j.psep.2017.10.007.

[8] Liu, Y., Zhou, S., Yang, F., Qin, H. & Kong, Y., *Degradation of Phenol in Industrial Wastewater over the F–Fe/TiO_2 Photocatalysts Under Visible Light Illumination*. Chinese Journal of Chemical Engineering, **24**(12), pp. 1712-1718, 2016. doi: 10.1016/j.cjche.2016.05.024.

[9] Saputera, W.H., Amri, A.F., Daiyan, R. & Sasongko, D., *Photocatalytic Technology for Palm Oil Mill Effluent (POME) Wastewater Treatment: Current Progress and Future Perspective*. Materials, **14**(11), 2846, 2021. doi: 10.3390/ma14112846.

[10] Muangpratoom, P., *The Effect of Temperature on the Electrical Characteristics of Nanofluids Based on Palm Oil*. Journal of Engineering and Technological Sciences, **53**(3), pp. 554-564, 2021. doi: 10.5614/j.eng.technol.sci.2021.53.3.12.

[11] Nurhayati, C., Susilawati, N., Susanto, T., Marthalia, W., Nugroho, A.K. & Pane, A.P., *The Effect of Linear Low-Density Polyethylene and Palm Kernel Shell Ash Mixture on the Physical, Mechanical and Degradation Properties of Paving Blocks*. Journal of Engineering and Technological Sciences, **54**(3), pp. 531-547, 2022. doi: 10.5614/j.eng.technol.sci.2022.54.3.7.

DOI: 10.5614/j.eng.technol.sci.2023.55.4.6

[12] Monsef, R., Ghiyasiyan-Arani, M. & Salavati-Niasari, M., *Design of Magnetically Recyclable Ternary $Fe_2O_3/EuVO_4/g\text{-}C_3N_4$ Nanocomposites for Photocatalytic and Electrochemical Hydrogen Storage*, ACS Applied Energy Materials, **4**(1), pp. 680-695, 2021. doi: 10.1021/acsaem.0c02557.

[13] Karami, A., Monsef, R., Shihan, M.R., Qassem, L.Y., Falah, M.W. & Salavati-Niasari, M., *UV-Light-Induced Photocatalytic Response of Pechini Sol-Gel Synthesized Erbium Vanadate Nanostructures Toward Degradation of Colored Pollutants*. Environmental Technology & Innovation, **28**, 102947, 2022. doi: 10.1016/j.eti.2022.102947.

[14] Panahi, A., Monsef, R., Imran, M.K., Mahdi, A.A., Ruhaima, A.A.K. & Salavati-Niasari, M., *$TmVO_4/Fe_2O_3$ Nanocomposites: Sonochemical Synthesis, Characterization, and Investigation of Photocatalytic Activity*, International Journal of Hydrogen Energy, **48**(10), pp. 3916-3930, 2023. doi: 10.1016/j.ijhydene.2022.10.226.

[15] Lendzion-Bieluń, Z., Wojciechowska, A., Grzechulska-Damszel, J., Narkiewicz, U., Śniadecki, Z. & Idzikowski, B., *Effective Processes o Phenol Degradation On Fe_3O_4-TiO_2 Nanostructured Magnetic Photocatalyst*. Journal of Physics and Chemistry of Solids, **136**, pp. 109178, 2020. doi: 10.1016/j.jpcs.2019.109178.

[16] Matos, J., Ocares-Riquelme, J., Poon, P.S., Montaña, R., García, X., Campos, K., Hernández-Garrido, J.C. & Titirici, M.M., *C-Doped Anatase TiO_2: Adsorption Kinetics and Photocatalytic Degradation of Methylene Blue and Phenol and Correlations with DFT Estimations*, Journal of Colloid and Interface Science, **547**, pp. 14-29, 2019. doi: 10.1016/j.jcis.2019.03.074.

[17] Saputera, W.H., Egiyawati, C., Putrie, A.S., Amri, A.F., Rizkiana, J. & Sasongko, D., *Titania Modified Silica from Sugarcane Bagasse Waste for Photocatalytic Wastewater Treatment*, IOP Conference Series: Materials Science and Engineering, **1143**(1), pp. 012073, 2021. doi: 10.1088/1757-899X/1143/1/012073.

[18] Hamdy, M.S., Saputera, W.H., Groenen, E.J. & Mul, G., *A novel TiO_2 Composite for Photocatalytic Wastewater Treatment*, Journal of Catalysis, **310**, pp. 75-83, 2014. DOI: 10.1016/j.jcat.2013.07.017.

[19] Saputera, W.H., Mul, G. & Hamdy, M.S., *Ti^{3+}-containing titania: Synthesis Tactics and Photocatalytic Performance*. Catalysis Today, **246**, pp. 60-66, 2015. doi: 10.1016/j.cattod.2014.07.049.

[20] Ho, T.N.S., Nguyen, T.T., Pham, T.H.T., Ngo, M.T. & Le, M.V., *Photocatalytic Degradation of Phenol in Aqueous Solutions Using TiO_2/SiO_2 Composite*, Chemical Engineering Transactions, **78**, pp. 427-432, 2020. DOI: 10.3303/CET2078072.

[21] Salavati-Niasari, M. & Amiri, A., *Synthesis and Characterization Of Alumina-Supported Mn(II), Co(II), Ni(II) And Cu(II) Complexes of Bis(Salicylaldiminato)Hydrazone as Catalysts for Oxidation of Cyclohexene With Tert-Buthylhydroperoxide*. Applied Catalysis A: General, **290**(1), pp. 46-53, 2005. doi: 10.1016/j.apcata.2005.05.009.

[22] Salavati-Niasari, M., *Zeolite-Encapsulation Copper(II) Complexes with 14-Membered Hexaaza Macrocycles: Synthesis, Characterization and Catalytic Activity*. Journal of Molecular Catalysis A: Chemical, **217**(1), pp. 87-92, 2004. doi: 10.1016/j.molcata.2004.02.022

[23] Salavati-Niasari, M., Ghanbari, D. & Davar, F., *Shape Selective Hydrothermal Synthesis of Tin Sulfide Nanoflowers Based On Nanosheets in The Presence of Thioglycolic Acid*, Journal of Alloys and Compounds, 492(1), pp. 570-575, 2010. doi: 10.1016/j.jallcom.2009.11.183.

[24] Monsef, R., Ghiyasiyan-Arani, M. & Salavati-Niasari, M., *Application of Ultrasound-Aided Method for the Synthesis of $NdVO_4$ Nano-Photocatalyst and Investigation of Eliminate Dye in Contaminant Water*, Ultrasonics Sonochemistry, **42**, pp. 201-211, 2018. doi: 10.1016/j.ultsonch.2017.11.025

[25] Amiri, M., Eskandari, K. & Salavati-Niasari, M., *Magnetically Retrievable Ferrite Nanoparticles in the Catalysis Application*, Advances in Colloid and Interface Science, **271**, 101982, 2019. doi: 10.1016/j.cis.2019.07.003.

[26] Irmawati, Y. Manzalini, S., Sugeng, B., Sudirman, Asahara, H. & Yudianti, R., *Microwave-assisted Synthesis of Functionalized Multiwalled Carbon Nanotube–Titanium Dioxide Hybrid Structure and Photodegradation*, Journal of Engineering and Technological Sciences, **54**(4), pp. 744-756, 2022. doi: 10.5614/j.eng.technol.sci.2022.54.4.7.

[27] Acosta-Herazo, R., Cañaveral-Velásquez, B., Pérez-Giraldo, K., Mueses, M.A., Pinzón-Cárdenas, M.H. & Machuca-Martínez, F., *A MATLAB-Based Application for Modeling and Simulation of Solar Slurry Photocatalytic Reactors for Environmental Applications*, Water, **12**(8), 2196, 2020. doi: 10.3390/w12082196.

[28] Finlayson-Pitts, B.J. & J.N. Pitts., Chapter 1 – Overview of the Chemistry of Polluted and Remote Atmospheres, in Chemistry of the Upper and Lower Atmosphere, B.J. Finlayson-Pitts and J.N. Pitts, Editors. 2000, Academic Press: San Diego. pp. 1-14.

[29] Malekshoar, G., Pal, K., He, Q., Yu, A. & Ray, A.K., *Enhanced Solar Photocatalytic Degradation of Phenol with Coupled Graphene-Based Titanium Dioxide and Zinc Oxide*, Industrial & Engineering Chemistry Research, **53**, pp. 18824-18832, 2014. doi: 10.1021/ie501673v.

[30] Górska, P., Zaleska, A., Suska, A. & Hupka, J., *Photocatalytic Activity and Surface Properties of Carbon-Doped Titanium Dioxide*, Physicochemical Problems of Mineral Processing, **43**, pp. 21-30, 2009.

[31] Zielińska, A., Kowalska, E., Sobczak, J.W., Łącka, I., Gazda, M., Ohtani, B., Hupka, J. & Zaleska, A., *Silver-Doped TiO_2 Prepared by Microemulsion Method: Surface Properties, Bio- And Photoactivity*. Separation and Purification Technology, 72(3), pp. 309-318, 2010. doi: 10.1016/j.seppur.2010.03.002

[32] Liu, S. & Chen, Z., *A Visible Light Response TiO_2 Photocatalyst Realized by Cationic S-Doping and Its Application for Phenol Degradation*, Journal of Hazardous Materials, **152**(1), pp. 48-55, 2008. doi: 10.1016/j.jhazmat.2007.06.062.

[33] Kang, X., Song, X.Z., Han, Y., Cao, J. & Tan, Z., *Defect-Engineered TiO_2 Hollow Spiny Nanocubes for Phenol Degradation under Visible Light Irradiation*. Scientific Reports, **8**(1), 5904, 2018. doi: 10.1038/s41598-018-24353-8.

[34] Yu, S., Yun, H.J., Kim, Y.H. & Yi, J., *Carbon-doped TiO_2 Nanoparticles Wrapped with Nanographene as A High Performance Photocatalyst for Phenol Degradation under Visible Light Irradiation*, Applied Catalysis B: Environmental, **144**, pp. 893-899, 2014. doi: 10.1016/j.apcatb.2013.08.030.

[35] Deng, Y., Xiao, Y., Zhou, Y., Zeng, T., Xing, M. & Zhang, J., *A Structural Engineering-Inspired Cds Based Composite for Photocatalytic Remediation of Organic Pollutant and Hexavalent Chromium*, Catalysis Today, **335**, pp. 101-109, 2019. doi: 10.1016/j.cattod.2018.09.012.

[36] Portela, R., Suárez, S., Tessinari, R.F., Hernández-Alonso, M.D., Canela, M.C. & Sánchez, B., *Solar/Lamp-Irradiated Tubular Photoreactor for Air Treatment with Transparent Supported Photocatalysts*, Applied Catalysis B: Environmental, **105**(1), pp. 95-102, 2011. doi: 10.1016/j.apcatb.2011.03.039.

[37] Ochoa-Gutiérrez, K.S., Tabare-Aguilar, E., Mueses, M.Á., Machuca-Martínez, F. & Puma, G.L., *A Novel Prototype Offset Multi Tubular Photoreactor (OMTP) for Solar Photocatalytic Degradation of Water Contaminants*, Chemical Engineering Journal, **341**, pp. 628-638, 2018. doi: 10.1016/j.cej.2018.02.068.

[38] Sutisna, Rokhmat, M., Wibowo, E., Khairurrijal & Abdullah, M., *Prototype of a Flat-Panel Photoreactor Using TiO_2 Nanoparticles Coated On Transparent Granules for The Degradation of Methylene Blue Under Solar Illumination*, Sustainable Environment Research, **27**(4), pp. 172-180, 2017. doi: 10.1016/j.serj.2017.04.002.

[39] Acosta-Herazo, R., Monterroza-Romero, J., Mueses, M.Á., Machuca-Martínez, F., Puma, G.L., *Coupling the Six Flux Absorption–Scattering Model to the Henyey–Greenstein Scattering Phase Function: Evaluation and Optimization of Radiation Absorption in Solar Heterogeneous Photoreactors*, Chemical Engineering Journal, **302**, pp. 86-96, 2016. doi: 10.1016/j.cej.2016.04.127.

[40] Wardhani, S., Purwonugroho, D., Fitri, C.W. & Prananto, Y.P., *Effect of pH and Irradiation Time on TiO_2-Chitosan Activity for Phenol Photo-Degradation*, AIP Conference Proceedings, **2021**(1), 2018. doi: 10.1063/1.5062759

[41] Onkani, S.P., Diagboya, P.N., Mtunzi, F.M., Klink, M.J., Olu-Owolabi, B.I. & Pakade, V., *Comparative Study of the Photocatalytic Degradation of 2–Chlorophenol Under UV Irradiation Using Pristine and Ag-Doped Species of TiO2, ZnO and ZnS Photocatalysts*, Journal of Environmental Management, **260**, pp. 110145, 2020. doi: 10.1016/j.jenvman.2020.110145.

[42] Pan, G., D. Wang, & Liu, Y., *Photocatalytic Degradation Pathways and Adsorption Modes of H-Acid in TiO_2 Suspensions*, Chinese Science Bulletin, **57**(10), pp. 1102-1108, 2012. DOI: 10.1007/s11434-011-4894-0.

[43] Chowdhury, P., Moreira, J., Gomaa, H. & Ray, A.K., *Visible-Solar-Light-Driven Photocatalytic Degradation of Phenol with Dye-Sensitized TiO_2: Parametric and Kinetic Study*, Industrial & Engineering Chemistry Research, **51**(12), pp. 4523-4532, 2012. doi: 10.1021/ie2025213.

[44] Reza, K.M., Kurny, A.S.W. & Gulshan, F., *Parameters Affecting the Photocatalytic Degradation of Dyes Using TiO_2: A Review*, Applied Water Science, **7**, pp. 1569-1578, 2017. doi: 10.1007/s13201-015-0367-y.

[45] Dong, S., Feng, J., Fan, M., Pi, Y., Hu, L., Han, X., Liu, M., Sun, J. & Sun, J., *Recent Developments in Heterogeneous Photocatalytic Water Treatment Using Visible Light-Responsive Photocatalysts: A Review*. RSC Advances, **5**, pp. 14610-14630, 2015. doi: 10.1039/C4RA13734E.

DOI: 10.5614/j.eng.technol.sci.2023.55.4.6

[46] Abdullah, A.M., Al-Thani, N.J., Tawbi, K. & Al-Kandari, H., *Carbon/Nitrogen-Doped TiO_2: New Synthesis Route, Characterization and Application for Phenol Degradation*, Arabian Journal of Chemistry, **9**(2), pp. 229-237, 2016. doi: 10.1016/j.arabjc.2015.04.027.

[47] Ungan, H. & Tekin, T., *Effect of the Sonication and Coating Time on the Photocatalytic Degradation of TiO_2, TiO_2-Ag, And TiO_2-Zno Thin Film Photocatalysts*, Chemical Engineering Communications, **207**(7), pp. 896-903, 2020. doi: 10.1080/00986445.2019.1630395.

[48] Zhai, H., Qi, J., Zhang, X., Li, H., Yang, L., Hu, C., Liu, H. & Yang, J., *Preparation and Photocatalytic Performance of Hollow Structure $LiNb_3O_8$ Photocatalysts*, Nanoscale Research Letters, **12**(1), pp. 519, 2017. doi: 10.1186/s11671-017-2291-6.

[49] Khayyat, S.A., Selvin, R., Roselin, L.S. & Umar, A., *Photocatalytic Oxidation of Phenolic Pollutants and Hydrophobic Organic Compounds in Industrial Wastewater Using Modified Nanosize Titanium Silicate-1 Thin Film Technology*, Journal of Nanoscience and Nanotechnology, **14**(9), pp. 7345-7350, 2014. doi: 10.1166/jnn.2014.9237.

[50] Khlyustova, A., Sirotkin, N., Kusova, T., Kraev, A., Titov, V. & Agafonov, A., *Doped TiO_2: The Effect of Doping Elements on Photocatalytic Activity*, Materials Advances, **1**(5), pp. 1193-1201, 2020. doi: 10.1039/D0MA00171F.

[51] Dozzi, M.V. & Selli, E., *Doping TiO_2 with p-Block Elements: Effects on Photocatalytic Activity*, Journal of Photochemistry and Photobiology C: Photochemistry Reviews, **14**, pp. 13-28, 2013. doi: 10.1016/j.jphotochemrev.2012.09.002.

[52] Carp, O., Huisman, C.L. & Reller, A., *Photoinduced Reactivity of Titanium Dioxide*. Progress in Solid State Chemistry, **32**(1), pp. 33-177, 2004. doi: 10.1016/j.progsolidstchem.2004.08.001.

[53] Mueses, M.A., Machuca-Martinez, F. & Puma, G.L., *Effective Quantum Yield and Reaction Rate Model for Evaluation of Photocatalytic Degradation of Water Contaminants in Heterogeneous Pilot-Scale Solar Photoreactors*. Chemical Engineering Journal, **215-216**, pp. 937-947, 2013. doi: 10.1016/j.cej.2012.11.076.